

# Hypernuclear constraints on the existence and lifetime of a deeply bound $H$ dibaryon

Avraham Gal\*

*Racah Institute of Physics, The Hebrew University, Jerusalem 9190401, Israel*

---

## Abstract

We study to what extent the unique observation of  $\Lambda\Lambda$  hypernuclei by their weak decay into known  $\Lambda$  hypernuclei, with lifetimes of order  $10^{-10}$  s, rules out the existence of a deeply bound doubly-strange ( $\mathcal{S}=-2$ )  $H$  dibaryon. Treating  ${}_{\Lambda\Lambda}^6\text{He}$  (the Nagara emulsion event) in a realistic  $\Lambda - \Lambda - {}^4\text{He}$  three-body model, we find that the  ${}_{\Lambda\Lambda}^6\text{He} \rightarrow H + {}^4\text{He}$  strong-interaction lifetime increases beyond  $10^{-10}$  s for  $m_H < m_\Lambda + m_n$ , about 176 MeV below the  $\Lambda\Lambda$  threshold, so that such a deeply bound  $H$  is not in conflict with hypernuclear data. Constrained by  $\Lambda$  hypernuclear  $\Delta\mathcal{S}=1$  nonmesonic weak-interaction decay rates, we evaluate the  $\Delta\mathcal{S}=2$   $H \rightarrow nn$  weak-decay lifetime of  $H$  in the mass range  $2m_n \lesssim m_H < m_\Lambda + m_n$ . The resulting  $H$  lifetime is of order  $10^4$  s, many orders of magnitude shorter than required to qualify for a dark-matter candidate. A lower-mass absolutely stable  $H$ ,  $m_H \lesssim 2m_n$ , is likely to be ruled out by established limits of nuclear stability such as for  ${}^{16}\text{O}$ .

---

## 1. Introduction

The deuteron, with mass only 2.2 MeV below the sum of masses of its proton and neutron constituents, is the only particle-stable six-quark (hexaquark) dibaryon known so far. Here stability is regarded with respect to the lifetime of the proton, many orders of magnitude longer than the lifetime of the Universe (13.8 billion years [1]). Extending the very-light  $ud$  quark sector by the light strange quark  $s$ , Lattice-QCD (LQCD) calculations suggest two strong-interaction stable hexaquarks. Both are  $J^\pi=0^+$  near-threshold  $s$ -wave dibaryons with zero spin and isospin: (i) a maximally strange  $\mathcal{S}=-6$

---

\*Avraham Gal, avragal@savion.huji.ac.il

$ssssss$  hexaquark classified as  $\Omega\Omega$  dibaryon member of the  $SU(3)$  flavor  $\mathbf{28}_f$  multiplet, and (ii) a strangeness  $\mathcal{S}=-2$   $uuddss$  hexaquark, a  $\mathbf{1}_f$   $H$  dibaryon, which is the subject of the present study. Whereas the LQCD calculation of  $\Omega\Omega$  reached  $m_\pi$  values close to the physical pion mass [2], the most recent  $H$  LQCD calculation [3] was done at  $m_\pi \approx 420$  MeV and within the  $SU(3)_f$  symmetry limit, where

$$H = -\sqrt{\frac{1}{8}}\Lambda\Lambda + \sqrt{\frac{3}{8}}\Sigma\Sigma + \sqrt{\frac{4}{8}}N\Xi. \quad (1)$$

It is likely that in the  $SU(3)_f$ -broken physical world a slightly bound  $\mathbf{1}_f$   $H$  becomes unbound with respect to the  $\Lambda\Lambda$  threshold, lying possibly a few MeV below the  $N\Xi$  threshold [4, 5].

The  $H$  dibaryon was predicted in 1977 by Jaffe [6] to lie about 80 MeV below the  $2m_\Lambda=2231$  MeV  $\Lambda\Lambda$  threshold. Dedicated experimental searches, beginning as soon as 1978 with a  $pp \rightarrow K^+K^-X$  reaction [7] at BNL, have failed to observe a  $\mathcal{S}=-2$  dibaryon signal over a wide range of dibaryon masses below  $2m_\Lambda$  [8, 9, 10], notably BABAR's recent search at SLAC looking for a  $\Upsilon(2S, 3S) \rightarrow \bar{\Lambda}\Lambda X$  decay [10]. Furthermore, a simple argument questioning the existence of a strong-interaction stable  $\mathcal{S}=-2$  dibaryon was put forward by several authors, notably Dalitz et al. [11]. It relates to the few established  $\Lambda\Lambda$  hypernuclei [12, 13], foremost the lightest known one  ${}_{\Lambda\Lambda}^6\text{He}$  (the Nagara emulsion event) where a  $\Lambda\Lambda$  pair is bound to  ${}^4\text{He}$  by  $6.91\pm 0.17$  MeV [14] exceeding twice the separation energy of a single  $\Lambda$  in  ${}^5_\Lambda\text{He}$  by merely  $\Delta B_{\Lambda\Lambda}({}_{\Lambda\Lambda}^6\text{He})=0.67\pm 0.17$  MeV. If  $H$  existed deeper than about 7 MeV below the  $\Lambda\Lambda$  threshold,  ${}_{\Lambda\Lambda}^6\text{He}$  could decay *strongly*,

$${}_{\Lambda\Lambda}^6\text{He} \rightarrow {}^4\text{He} + H, \quad (2)$$

considerably faster than the  $\Delta\mathcal{S}=1$  *weak-interaction* decay by which it has been observed and uniquely identified [14]:

$${}_{\Lambda\Lambda}^6\text{He} \rightarrow {}^5_\Lambda\text{He} + p + \pi^-. \quad (3)$$

Further arguments questioning an  $H$  bound by less than about 7 MeV were put forward by Gal [15].

Arguments of this kind, questioning the existence of a strong-interaction stable  $H$  dibaryon, were challenged 20 years ago by Farrar [16] who suggested that the  $H$  dibaryon may be a long-lived compact object with as small radius as 0.2 fm and as small mass as  $1.5\pm 0.2$  GeV, in which case it becomes

absolutely stable, without disrupting the observed stability of nuclei. Once sufficiently abundant, relic  $H$  dibaryons would qualify as a cold Dark Matter (DM) candidate. Farrar’s present estimate for the mass  $m_H$  of such a compact dibaryon, often termed Sexaquark in these works, is between 1850 and 2050 MeV [17], where  $m_H < 1800$  MeV is disfavored by the stability of deuterium. Here, the uppermost mass value 2050 MeV stems from the threshold value  $(m_n + m_\Lambda) = 2055$  MeV, above which the  $\Delta\mathcal{S}=1$  strangeness changing weak decay  $H \rightarrow \Lambda n$  would make  $H$  short lived with respect to a lifetime of cosmological origin expected for a DM candidate. For a recent discussion of this suggestion and its possibly intriguing consequences, see Ref. [17].

Following Farrar’s conjecture of a deeply-bound compact  $\mathcal{S}=-2$  dibaryon, we present a realistic calculation of  ${}_{\Lambda\Lambda}^6\text{He}$  lifetime owing to the two-body strong-interaction decay reaction Eq. (2). Treating  ${}_{\Lambda\Lambda}^6\text{He}$  in a  $\Lambda - \Lambda - {}^4\text{He}$  three-body model, it is found that the  ${}_{\Lambda\Lambda}^6\text{He} \rightarrow H + {}^4\text{He}$  strong-interaction lifetime is correlated strongly with  $m_H$ , increasing upon decreasing  $m_H$  such that it exceeds the hypernuclear  $\Delta\mathcal{S}=1$  weak-decay lifetime scale of order  $10^{-10}$  s for  $m_H < m_\Lambda + m_n$ . Constrained by  $\Lambda$  hypernuclear  $\Delta\mathcal{S}=1$  non-mesonic weak-interaction decay rates within leading-order (LO) effective field theory (EFT) approach, we present a realistic calculation of the  $\Delta\mathcal{S}=2$  weak decay  $H \rightarrow nn$  for  $(m_n + m_\Lambda) > m_H \gtrsim 2m_n$ , resulting in  $H$  lifetimes of order  $10^4$  s, 11 orders of magnitude shorter than the order of  $10^8$  yr reached in the 2004 calculation by Farrar and Zaharijas (FZ) [18]. Hence, a deeply bound  $H$  dibaryon would be far from qualifying for a DM candidate.

## 2. $H$ dibaryon wavefunction

### 2.1. Spatial part

Here we follow the simple ansatz for the  $H$  dibaryon six-quark ( $6q$ ) fully symmetric spatial wavefunction  $\Psi_H$  given by FZ [18]:

$$\Psi_H = N_6 \exp\left(-\frac{\nu}{6} \sum_{i<j}^6 (\mathbf{r}_i - \mathbf{r}_j)^2\right), \quad (4)$$

where  $N_6$  is a normalization constant and  $\nu$  is related to the  $H$  ‘size’ as detailed below. To transform this  $6q$   $\Psi_H$  to a two-baryon form where each baryon  $B_a$  and  $B_b$  is described as a  $3q$  cluster, we define relative coordinates  $\boldsymbol{\rho}$ ,  $\boldsymbol{\lambda}$  and center-of-mass (c.m.) coordinates  $\mathbf{R}$ :

$$B_a: \quad \boldsymbol{\rho}_a = \mathbf{r}_2 - \mathbf{r}_1, \quad \boldsymbol{\lambda}_a = \mathbf{r}_3 - \frac{1}{2}(\mathbf{r}_1 + \mathbf{r}_2), \quad \mathbf{R}_a = \frac{1}{3}(\mathbf{r}_1 + \mathbf{r}_2 + \mathbf{r}_3), \quad (5)$$

$$B_b: \quad \boldsymbol{\rho}_b = \mathbf{r}_5 - \mathbf{r}_4, \quad \boldsymbol{\lambda}_b = \mathbf{r}_6 - \frac{1}{2}(\mathbf{r}_4 + \mathbf{r}_5), \quad \mathbf{R}_b = \frac{1}{3}(\mathbf{r}_4 + \mathbf{r}_5 + \mathbf{r}_6), \quad (6)$$

plus a total cm coordinate  $\mathbf{R} = \frac{1}{2}(\mathbf{R}_a + \mathbf{R}_b) = \frac{1}{6} \sum_i^6 \mathbf{r}_i$ . Using these  $\boldsymbol{\rho}$  and  $\boldsymbol{\lambda}$  intrinsic quark coordinates, plus a relative coordinate  $\mathbf{r} = (\mathbf{R}_b - \mathbf{R}_a)$  between the baryonic  $3q$  clusters  $B_a$  and  $B_b$ , Eq. (4) assumes the form

$$\Psi_H = \psi_{B_a}(\boldsymbol{\rho}_a, \boldsymbol{\lambda}_a) \times \psi_{B_b}(\boldsymbol{\rho}_b, \boldsymbol{\lambda}_b) \times \psi_{B_a B_b}(\mathbf{r}), \quad (7)$$

where

$$\psi_{B_j} = \left( \frac{4\nu^2}{3\pi^2} \right)^{\frac{3}{4}} \exp\left(-\frac{\nu}{2}\rho_j^2 - \frac{2\nu}{3}\lambda_j^2\right) \quad (8)$$

provides normalized  $3q$  baryonic spatial wf for baryon  $B_j$ ,  $j = a, b$ , and

$$\psi_{B_a B_b} = \left( \frac{3\nu}{\pi} \right)^{\frac{3}{4}} \exp\left(-\frac{3\nu}{2}r^2\right) \quad (9)$$

provides a normalized spatial wavefunction in the relative coordinate  $\vec{r}$  of the dibaryon  $B_a B_b$ . Note that all three components of  $H$  in Eq. (7) share the *same* root-mean-square (r.m.s.) radius value:

$$\langle r_{B_a}^2 \rangle = \langle r_{B_b}^2 \rangle = \langle r_{B_a B_b}^2 \rangle = \frac{9}{8\nu}, \quad (10)$$

while for  $\Psi_H$  it is given by

$$\langle r_H^2 \rangle = \frac{5}{8\nu} \quad (11)$$

(correcting an error:  $\langle r_H^2 \rangle = \nu^{-1}$  in Ref. [18]), so that the radial extent of  $H$  is about 75% of the radial extent of each of its three components  $B_a, B_b, B_a B_b$ . We also note that a  $3q$  baryon wavefunction, similar to  $\Psi_H$  for  $6q$ ,

$$\Psi_B = N_3 \exp\left(-\frac{\nu}{6} \sum_{i<j}^3 (\mathbf{r}_i - \mathbf{r}_j)^2\right), \quad (12)$$

implies a r.m.s. radius squared of

$$\langle r_B^2 \rangle = \frac{1}{\nu}, \quad (13)$$

slightly smaller according to Eq. (10) than when embedded within the  $H$  dibaryon.

Table 1:  $\sqrt{\langle r_{\Lambda\Lambda}^2 \rangle}$  (fm units) vs.  $B_{\Lambda\Lambda}$  (MeV units) for a short-range Gaussian  $\Lambda\Lambda$  potential, Eq. (14) with  $\lambda = 4 \text{ fm}^{-1}$ . I'm indebted to Martin Schäfer for providing me with this table.

$B_{\Lambda\Lambda}$	5	20	50	100	200	300	400	1000
$\sqrt{\langle r_{\Lambda\Lambda}^2 \rangle}$	2.134	1.206	0.854	0.689	0.560	0.501	0.463	0.366

Although derived for a specific spatially *symmetric* wavefunction, Eq. (4), the relationships noted above between various  $\langle r^2 \rangle$  values hold for *any* spatially symmetric form chosen for  $H$ . Establishing physically one such ‘size’ value determines necessarily all other ‘size’ values. However, the choice of a specific ‘size’ value is constrained by the choice of  $H$  binding energy value, as demonstrated in Table 1 for  $B_a = B_b = \Lambda$ . In this particular case, the Schroedinger equation in the relative coordinate  $\mathbf{r}_{\Lambda\Lambda}$  was solved for assumed binding energy values  $B_{\Lambda\Lambda}$ , using attractive Gaussian  $\Lambda\Lambda$  potential of the form  $C_0^{(\lambda)}\delta_\lambda(\mathbf{r})$ , where  $C_0^{(\lambda)}$  is a strength parameter fitted to given values of  $B_{\Lambda\Lambda}$  and

$$\delta_\lambda(\mathbf{r}) = \left(\frac{\lambda}{2\sqrt{\pi}}\right)^3 \exp\left(-\frac{\lambda^2}{4}\mathbf{r}^2\right) \quad (14)$$

is a zero-range Dirac  $\delta^{(3)}(\mathbf{r})$  function in the limit  $\lambda \rightarrow \infty$ , smeared over distance of  $\sqrt{\langle r^2 \rangle_\lambda} = \sqrt{6}/\lambda$  (0.612 fm for  $\lambda = 4 \text{ fm}^{-1}$  chosen here). As expected, once  $B_{\Lambda\Lambda}$  increases beyond a nuclear physics scale of roughly 20 MeV or so,  $\sqrt{\langle r_{\Lambda\Lambda}^2 \rangle}$  decreases below 1 fm down to  $\approx 0.5$  fm. The corresponding  $H$  r.m.s. radius values are even smaller:  $\sqrt{\langle r_H^2 \rangle}/\sqrt{\langle r_{\Lambda\Lambda}^2 \rangle} = (\sqrt{5}/3) \approx 0.745$  according to Eqs. (10,11). Taking a shorter-range Gaussian potential, say with  $\lambda = 5 \text{ fm}^{-1}$ , has a relatively small effect on  $\sqrt{\langle r_{\Lambda\Lambda}^2 \rangle}$  which decreases between 3% to 12% as  $B_{\Lambda\Lambda}$  increases from 5 to 1000 MeV. In passing we comment that the constraint imposed on  $\sqrt{\langle r_H^2 \rangle}$  by assuming a definite value of  $B_{\Lambda\Lambda}$ , or vice versa, was overlooked in Ref. [18].

In the calculations reported below we use the fully symmetric spatial  $H$  wavefunction (4) or equivalently (7) by choosing  $\nu = (9/8)\langle r_{\Lambda\Lambda}^2 \rangle^{-1}$ , see Eq. (10), where  $\langle r_{\Lambda\Lambda}^2 \rangle$  is obtained by solving the Schroedinger equation with attractive  $\Lambda\Lambda$  potential shape, Eq. (14) for  $\lambda = 4 \text{ fm}^{-1}$ , and variable strength determined by assuming given values of  $B_{\Lambda\Lambda}$ , as listed in Table 1.

## 2.2. Spin-Flavor-Color part

To complete the discussion of the  $H$  dibaryon wavefunction we note that the fully symmetric spatial  $6q$  wf  $\Psi_H$ , Eq. (4), needs to be supplemented by a singlet  $\mathbf{1}_S$  total spin  $S=0$  component, represented by a  $6q$  SU(2) Young tableau

$$\begin{array}{|c|c|c|} \hline & & \\ \hline & & \\ \hline \end{array} \quad , \quad (15)$$

and by singlet  $\mathbf{1}_F$  total flavor ( $F$ ) and  $\mathbf{1}_C$  total color ( $C$ ) components, each represented by its own  $6q$  SU(3) Young tableau

$$\begin{array}{|c|c|} \hline & \\ \hline & \\ \hline & \\ \hline \end{array} \quad . \quad (16)$$

$F$  or  $C$

Each of these  $S$ ,  $F$  and  $C$  tableaux accommodates five components. In spin space, only one component corresponds to  $S_a(uds) = S_b(uds) = \frac{1}{2}$  and  $S_a(ud) = S_b(ud) = 0$  implied by a  $\Lambda\Lambda$  dibaryon component, and in flavor space, again, only one component corresponds to  $\mathbf{8}_a(uds)$  and  $\mathbf{8}_b(uds)$  with isospin  $I_a(ud) = I_b(ud) = 0$  for a  $\Lambda\Lambda$  dibaryon component. In color space, too, only one component corresponds to colorless  $\mathbf{1}_a(uds)$  and  $\mathbf{1}_b(uds)$  baryons. Hence, up to a phase, we assign in each of these three spaces a coefficient of fractional parentage  $\sqrt{1/5}$  to  $\Psi_H$  of Eq. (7). Finally, having chosen the  $\Lambda\Lambda$  component over the  $\Sigma\Sigma$  and  $N\Xi$  components of  $H$ , see Eq. (1), involves a Clebsch-Gordan coefficient of magnitude  $\sqrt{1/8}$  which together with the former coefficients amounts to supplementing the spatially symmetric  $\Lambda\Lambda$  wavefunction  $\psi_{\Lambda\Lambda}$ , Eq. (7) for  $B_a = B_b = \Lambda$ , by a flavor-color-spin factor  $\sqrt{1/1000}$ .

## 3. ${}_{\Lambda\Lambda}{}^6\text{He}$ wavefunction

### 3.1. Three-body approximation

Given the tight binding of  ${}^4\text{He}$ , we treat the six-body  ${}_{\Lambda\Lambda}{}^6\text{He}$  as a three-body  $\Lambda\Lambda\alpha$  system with spatial coordinates  $\mathbf{r}_\alpha$ ,  $\mathbf{r}_{\Lambda_1}$ ,  $\mathbf{r}_{\Lambda_2}$ . Starting from the two relative  $\Lambda\alpha$  vector coordinates  $\mathbf{r}_{\Lambda_1\alpha} = \mathbf{r}_{\Lambda_1} - \mathbf{r}_\alpha$  and  $\mathbf{r}_{\Lambda_2\alpha} = \mathbf{r}_{\Lambda_2} - \mathbf{r}_\alpha$ , we transform to their relative and c.m. coordinates

$$\mathbf{r}_{\Lambda\Lambda} = \mathbf{r}_{\Lambda_2\alpha} - \mathbf{r}_{\Lambda_1\alpha}, \quad \mathbf{R}_{\Lambda\Lambda} = \frac{1}{2}(\mathbf{r}_{\Lambda_1\alpha} + \mathbf{r}_{\Lambda_2\alpha}). \quad (17)$$

A reasonable simple approximation of the Pionless-EFT ( $\not\pi$ EFT)  ${}_{\Lambda\Lambda}{}^6\text{He}$  wavefunction calculated in Ref. [19] is then to use a factorized ansatz:

$$\Phi_{{}_{\Lambda\Lambda}{}^6\text{He}} = \phi_{\Lambda\Lambda}(r_{\Lambda\Lambda}) \Phi_{\Lambda\Lambda}(R_{\Lambda\Lambda}) \phi_{\alpha}, \quad (18)$$

where the wavefunctions  $\phi_{\Lambda\Lambda}$  and  $\Phi_{\Lambda\Lambda}$  are chosen as Gaussians constrained by requiring that  $\phi_{\Lambda\Lambda}$  reproduces the r.m.s. radius of the coordinate  $\mathbf{r}_{\Lambda\Lambda}$  in the 6-body  ${}_{\Lambda\Lambda}{}^6\text{He}$   $\not\pi$ EFT calculation [19] as discussed below. Finally, the  ${}^4\text{He}$  core wavefunction  $\phi_{\alpha}$  within  ${}_{\Lambda\Lambda}{}^6\text{He}$  is approximated by a free-space  ${}^4\text{He}$  wavefunction identical with the final-state  ${}^4\text{He}$  in the  ${}_{\Lambda\Lambda}{}^6\text{He} \rightarrow H + {}^4\text{He}$  strong-interaction decay.

Studying the  $\not\pi$ EFT  ${}^5_{\Lambda}\text{He}$  five-body calculation [20] we note that  $B_{\Lambda}^{\text{exp}}({}^5_{\Lambda}\text{He})$  is nearly reproduced by choosing Eq. (14) for  $\Lambda N$  contact terms, with cutoff values  $\lambda = 1.25 \text{ fm}^{-1}$  or  $\lambda = 1.50 \text{ fm}^{-1}$  for  $\Lambda N$  scattering length versions Alexander(B) and  $\chi$ EFT(NLO19). Going over to the  $\not\pi$ EFT  ${}_{\Lambda\Lambda}{}^6\text{He}$  six-body calculation [19], the  $\Lambda\Lambda$  r.m.s. distance computed for these cutoff values is  $\sqrt{\langle r_{\Lambda\Lambda}^2 \rangle} = 3.65 \pm 0.10 \text{ fm}$ , which we adopt for the r.m.s. radius of the Gaussian  $\phi_{\Lambda\Lambda}$  in Eq. (18). Note that  $\phi_{\Lambda\Lambda}$  appears as a bound-state wavefunction in spite of the  $\Lambda\Lambda$  interaction being much too weak to form a bound state; it is the  ${}^4\text{He}$  nuclear core that stabilizes the two  $\Lambda$ s in  ${}_{\Lambda\Lambda}{}^6\text{He}$ . To make sense of as large  $\sqrt{\langle r_{\Lambda\Lambda}^2 \rangle}$  value for  ${}_{\Lambda\Lambda}{}^6\text{He}$ , we refer to Hiyama's  ${}^5_{\Lambda}\text{He}$  calculation [21] where  $\sqrt{\langle r_{\Lambda\alpha}^2 \rangle} = 2.79 \text{ fm}$ . Assuming this same value for each  $\mathbf{r}_{\Lambda_j\alpha}$  ( $j = 1, 2$  in  ${}_{\Lambda\Lambda}{}^6\text{He}$ ) we get  $\sqrt{\langle r_{\Lambda\Lambda}^2 \rangle} \approx \sqrt{2 \langle r_{\Lambda\alpha}^2 \rangle} = \sqrt{2} \times 2.79 = 3.95 \text{ fm}$ , only 8% larger than the value  $3.65 \pm 0.10 \text{ fm}$  concluded above. We also note that since this value refers to a weakly 'bound'  $\Lambda\Lambda$  pair in  ${}_{\Lambda\Lambda}{}^6\text{He}$ , it is considerably larger than  $\sqrt{\langle r_{\Lambda\Lambda}^2 \rangle}$  values listed in Table 1 for a tightly bound  $H$  dibaryon. Finally, having accepted  $\sqrt{\langle r_{\Lambda\Lambda}^2 \rangle} = 3.65 \pm 0.10 \text{ fm}$  for the Gaussian  $\phi_{\Lambda\Lambda}$ , the r.m.s. radius value of the c.m. Gaussian  $\Phi_{\Lambda\Lambda}$  is half of that.

### 3.2. Short-range behavior

Eq. (18) provides a simple wavefunction for two loosely bound  $\Lambda$  hyperons held together by  ${}^4\text{He}$ , disregarding the short-range repulsive component of the  $\Lambda\Lambda$  interaction which is manifest in LQCD calculations [22] and is probed by a relatively compact  $H$  dibaryon. To check the effect exerted by short-range repulsion on the  ${}_{\Lambda\Lambda}{}^6\text{He} \rightarrow H + {}^4\text{He}$  decay rate, we modify  $\phi_{\Lambda\Lambda}$  in Eq. (18) by introducing a short-range correlation (SRC) factor  $[1 - j_0(\kappa r)]$ , where  $j_0$  is a

spherical Bessel function of order zero:

$$\tilde{\phi}_{\Lambda\Lambda}(r_{\Lambda\Lambda}) = (1 - j_0(\kappa r_{\Lambda\Lambda})) \phi_{\Lambda\Lambda}(r_{\Lambda\Lambda}). \quad (19)$$

Choosing  $\kappa = 2.534 \text{ fm}^{-1}$ , corresponding to 500 MeV/c in momentum space, nearly reproduces the  $\Lambda\Lambda$  NSC97  $G$ -matrix calculation in Ref. [23] (Fig. 2 there and related text). We therefore replace  $\Phi_{\Lambda\Lambda}^6\text{He}$ , Eq. (18), by

$$\Psi_i = \tilde{\phi}_{\Lambda\Lambda}(r_{\Lambda\Lambda}) \Phi_{\Lambda\Lambda}(R_{\Lambda\Lambda}) \phi_\alpha \quad (20)$$

for use as initial  ${}_{\Lambda\Lambda}^6\text{He}$  wavefunction in the  ${}_{\Lambda\Lambda}^6\text{He} \rightarrow H + {}^4\text{He}$  decay rate calculation reported below.

#### 4. ${}_{\Lambda\Lambda}^6\text{He} \rightarrow H + {}^4\text{He}$ decay rate

We assume that the strong-interaction decay  ${}_{\Lambda\Lambda}^6\text{He} \rightarrow H + {}^4\text{He}$  of a loosely ‘bound’  $\Lambda\Lambda$  pair in  ${}_{\Lambda\Lambda}^6\text{He}$  into a  $\Lambda\Lambda$  pair constituent of a tightly bound  $\mathbf{1}_F$   $H$  dibaryon, flying off  ${}^4\text{He}$  with momentum  $\mathbf{k}_H$  in their c.m. system, is triggered by the  $\Lambda\Lambda$  strong interaction  $V_{\Lambda\Lambda}$  extracted near threshold. The spatial dependence of the decay matrix element is given by  $\langle \Psi_f | V_{\Lambda\Lambda} | \Psi_i \rangle$ , where  $\Psi_i$  stands for the initial  ${}_{\Lambda\Lambda}^6\text{He}$  wavefunction, Eq. (20), and

$$\Psi_f = \tilde{\psi}_{\Lambda\Lambda}(r_{\Lambda\Lambda}) \exp(i\mathbf{k}_H \cdot \mathbf{R}_H) \phi_\alpha, \quad \tilde{\psi}_{\Lambda\Lambda} = \sqrt{1/1000} \times \psi_{\Lambda\Lambda}, \quad (21)$$

where  $\psi_{\Lambda\Lambda}$ , Eq. (9), is renormalized by the flavor-color-spin factor  $\sqrt{1/1000}$  discussed at the end of subsection 2.2, thereby accounting for the elimination of  $\Sigma\Sigma$  and  $N\Xi$  components of  $H$ . Note that in agreement with the overall attraction of the  $BB$  interaction in the  $\mathbf{1}_F$  channel [22] no SRC factor was introduced in Eq. (21) for  $\Psi_f$ . We note that the calculations reported below disregard the slight difference between the inner  $3q$  structure of each  $\Lambda$  hyperon in the  $H$  dibaryon to that in  ${}_{\Lambda\Lambda}^6\text{He}$ . For a  $3q$  baryon size of about 0.5 fm [24], this neglect is well justified in the range of  $B_{\Lambda\Lambda}$  values considered here.

The  ${}_{\Lambda\Lambda}^6\text{He} \rightarrow H + {}^4\text{He}$  decay rate, or equivalently the corresponding strong-interaction width of  ${}_{\Lambda\Lambda}^6\text{He}$ , is given by [25]:

$$\Gamma({}_{\Lambda\Lambda}^6\text{He} \rightarrow H + {}^4\text{He}) = \frac{\mu_{H\alpha} k_H}{(2\pi\hbar c)^2} \int |\langle \Psi_f | V_{\Lambda\Lambda} | \Psi_i \rangle|^2 d\hat{\mathbf{k}}_H, \quad (22)$$

where  $\mu_{H\alpha}$  is the  $H - {}^4\text{He}$  reduced mass and  $\langle \Psi_f | V_{\Lambda\Lambda} | \Psi_i \rangle$  is a product of two factors, as follows.

One factor is the  $\Lambda\Lambda$  interaction matrix element  $\langle \tilde{\psi}_{\Lambda\Lambda} | V_{\Lambda\Lambda} | \tilde{\phi}_{\Lambda\Lambda} \rangle$  in the  $r_{\Lambda\Lambda}$  relative distance with  $V_{\Lambda\Lambda}$  connecting  $\tilde{\phi}_{\Lambda\Lambda}$ , Eq. (19), for the initial  ${}_{\Lambda\Lambda}^6\text{He}$  wavefunction component to the final  $H$  dibaryon renormalized wavefunction component  $\tilde{\psi}_{\Lambda\Lambda}$ , Eq. (21). A normalized Gaussian  $\delta_{\lambda=4}(\mathbf{r})$ , see Eq. (14), was used for  $V_{\Lambda\Lambda}$  with strength parameter  $C_0^{(\lambda=4)} = -152 \text{ MeV}\cdot\text{fm}^3$  fitted in Ref. [19] to the HAL-QCD scattering length  $a_{\Lambda\Lambda} = -0.8 \text{ fm}$  [26]. The calculated matrix element  $\langle V_{\Lambda\Lambda} \rangle$  depends weakly on the chosen value of  $\lambda$  within  $\delta\lambda = \pm 1 \text{ fm}^{-1}$ . As for dependence on SRC, Eq. (19), it introduces a multiplicative factor

$$1 - \exp(-\kappa^2/4\chi) \quad (23)$$

to  $\langle V_{\Lambda\Lambda} \rangle$ , with  $\chi = \frac{1}{2}(\nu_i + \nu_f) + \frac{1}{4}\lambda^2$  for wavefunctions of Gaussian shape  $\exp(-\nu r^2/2)$ . This factor varies from 0.25 to 0.19 as  $B_{\Lambda\Lambda}$  is increased from 100 to 400 MeV. Altogether, the matrix element  $\langle \tilde{\psi}_{\Lambda\Lambda} | V_{\Lambda\Lambda} | \tilde{\phi}_{\Lambda\Lambda} \rangle$  varies slightly from  $-59$  to  $-53 \text{ keV}$  in the same  $B_{\Lambda\Lambda}$  range.

Table 2:  ${}_{\Lambda\Lambda}^6\text{He} \rightarrow H + {}^4\text{He}$  decay rate  $\Gamma$ , Eq. (22), and decay time  $\hbar/\Gamma$  for some representative values of  $H$  binding energy  $B_{\Lambda\Lambda}$  and their associated  $k_H$  and  $I(k_H; a_\Phi)$  values for  $a_\Phi = 1.49 \text{ fm}$ , see text.  $B_{\Lambda\Lambda} = 176 \text{ MeV}$  corresponds to  $m_H = m_\Lambda + m_n$ .

$B_{\Lambda\Lambda}$ (MeV)	$k_H$ ( $\text{fm}^{-1}$ )	$I(k_H; a_\Phi)$ ( $\text{fm}^3$ )	$\Gamma$ (eV)	$\tau = \hbar/\Gamma$ (s)
100	2.547	$1.002 \cdot 10^{-3}$	$0.782 \cdot 10^{-2}$	$0.841 \cdot 10^{-13}$
200	3.612	$4.742 \cdot 10^{-10}$	$0.501 \cdot 10^{-8}$	$1.315 \cdot 10^{-7}$
300	4.377	$5.996 \cdot 10^{-16}$	$0.679 \cdot 10^{-14}$	$0.970 \cdot 10^{-1}$
400	4.980	$2.157 \cdot 10^{-21}$	$2.436 \cdot 10^{-20}$	$2.703 \cdot 10^4$
176	3.393	$1.521 \cdot 10^{-8}$	$1.550 \cdot 10^{-7}$	$4.245 \cdot 10^{-9}$

The other factor in  $\langle \Psi_f | V_{\Lambda\Lambda} | \Psi_i \rangle$  is an overlap matrix element between the initial  $\Lambda\Lambda - \alpha$  Gaussian wavefunction  $\Phi_{\Lambda\Lambda}(R_{\Lambda\Lambda})$  in  ${}_{\Lambda\Lambda}^6\text{He}$  and the final outgoing  $H - \alpha$  plane-wave  $\exp(i\mathbf{k}_H \cdot \mathbf{R}_H)$ . Note that  $\mathbf{R}_H$  has nothing to do with the relatively small size of  $H$ . In the following we identify  $\mathbf{R}_H$  with the corresponding argument  $\mathbf{R}_{\Lambda\Lambda}$  in Eq. (18), both defined relative to  ${}^4\text{He}$  and denoted below simply by  $\mathbf{R}$ . The square of this overlap matrix element times  $4\pi$  from  $d\hat{\mathbf{k}}_H$  in Eq. (22) is given by

$$I(k_H; a_\Phi) \equiv 4\pi \left| \int \exp(i\mathbf{k}_H \cdot \mathbf{R}) \Phi_{\Lambda\Lambda}(R) d^3\mathbf{R} \right|^2 = 32\pi^{5/2} a_\Phi^3 \exp(-a_\Phi^2 k_H^2), \quad (24)$$

where  $a_\Phi = \sqrt{2 \langle R_{\Lambda\Lambda}^2 \rangle / 3} = 1.49 \pm 0.04$  fm. As shown in Table 2,  $I(k_H; a_\Phi)$  varies strongly with  $k_H$  over 18 decades as  $B_{\Lambda\Lambda}$  is varied from 100 MeV (76 MeV above  $m_\Lambda + m_n$ ) to 400 MeV (47 MeV below  $2m_n$ ). This is caused by the increased oscillations of  $\exp(i\mathbf{k}_H \cdot \mathbf{R})$  vs. the smoothly varying  $\Phi_{\Lambda\Lambda}(R)$  in Eq. (24). And on top of that, the  $\pm 0.04$  fm uncertainty of  $a_\Phi$  makes  $I(k_H; a_\Phi)$  uncertain by a factor of 4 larger/smaller values than for the mean value  $a_\Phi = 1.49$  fm at  $B_{\Lambda\Lambda} = 176$  MeV corresponding to the  $m_\Lambda + m_n$  threshold, increasing to a factor about 20 at  $B_{\Lambda\Lambda} = 400$  MeV.

The final values of  ${}_{\Lambda\Lambda}^6\text{He} \rightarrow H + {}^4\text{He}$  decay rate  $\Gamma$  listed in Table 2 account for the two factors in  $\langle \Psi_f | V_{\Lambda\Lambda} | \Psi_i \rangle$  considered above. Notably,  $\Gamma$  decreases over 17 decades, reflecting the strong variation of  $I(k_H; a_\Phi)$  with  $B_{\Lambda\Lambda}$ , and the  ${}_{\Lambda\Lambda}^6\text{He}$  strong-interaction lifetime  $\tau = \hbar/\Gamma$  increases as strongly over this range of  $B_{\Lambda\Lambda}$  values. In particular, for  $H$  binding energy  $B_{\Lambda\Lambda}$  somewhat lower than 176 MeV ( $m_\Lambda + m_n$  threshold),  $\tau$  starts to exceed the weak-interaction lifetime scale set by the free- $\Lambda$  lifetime  $\approx 2.6 \times 10^{-10}$  s, so that the robust observation of  $\Lambda\Lambda$  hypernuclei by their weak-interaction decay modes does not rule out the existence of a deeply bound  $H$  dibaryon with mass below  $m_\Lambda + m_n$ .

## 5. $\Lambda\Lambda$ nonmesonic weak decays

Having realized that a deeply bound  $H$  dibaryon lying below  $m_\Lambda + m_n$  is not in conflict with the weak-decay lifetime scale  $\sim 10^{-10}$  s of all observed  $\Lambda\Lambda$  hypernuclei, we now estimate the leading  $\Delta\mathcal{S} = 2$  weak-interaction decay rate of  $H$ , that of the  $H \rightarrow nn$  two-body decay.  $H$  is represented here, as above, by its deeply bound  $\Lambda\Lambda$  component. Although  $\Delta\mathcal{S} = 2$   $\Lambda\Lambda \rightarrow nn$  transitions are not constrained directly by experiment, they are related to  $\Delta\mathcal{S} = 1$   $\Lambda n \rightarrow nn$  transitions which are constrained by ample lifetime data in  $\Lambda$  hypernuclei [12]. These  $\Delta\mathcal{S} = 1$  transitions, including the pion-exchange transition depicted in Fig. 1(b), proceed in  $\Lambda$  hypernuclei with a total rate comparable to the  $\Lambda \rightarrow n\pi^0$  free-space decay rate associated with Fig. 1(a). The weak-interaction coupling constant  $g_w$  extracted from the free-space  $\Lambda$  lifetime, and proved to be relevant in the  $\Lambda n \rightarrow nn$  nonmesonic decay of  $\Lambda$  hypernuclei, could then be used as shown in Fig. 1(c) to estimate the strength of the  $\Delta\mathcal{S} = 2$   $\Lambda\Lambda \rightarrow nn$  weak-decay transition.

Pion exchange is not the only contributor to the nonmesonic weak decay of  $\Lambda$  hypernuclei. Owing to the large momentum transfer in Fig. 1(b), pion exchange generates mostly a tensor  ${}^3S_1 \rightarrow {}^3D_1$  transition which is Pauli

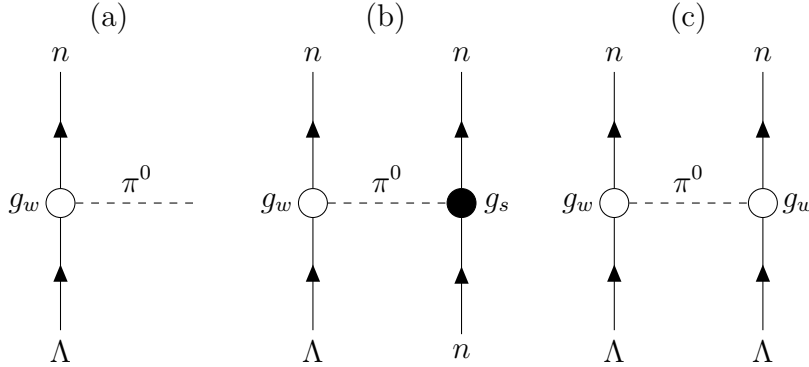


Figure 1:  $\Delta\mathcal{S} = 1$   $\Lambda \rightarrow n$  weak-interaction diagrams in free space (a) or in  $\Lambda$  hypernuclei (b), see Dalitz [27], and  $\Delta\mathcal{S} = 2$   $\Lambda\Lambda \rightarrow nn$  weak-interaction diagram (c), all involving emission (a) or exchange (b,c) of a  $\pi^0$  meson. Weak-interaction and strong-interaction coupling constants  $g_w$  and  $g_s$ , respectively, are denoted by circles.

forbidden for  $nn$  final states, so shorter-range meson exchanges contribute instead. It is useful then to follow an EFT approach initiated by Parreño et al. [28] and updated recently in Ref. [29]. In this approach, Fig. 1(b) and Fig. 1(c) are replaced by Fig. 2(a) and Fig. 2(b), respectively, where the square vertices stand at LO for  ${}^1S_0 \rightarrow {}^1S_0$  low-energy constants (LECs) that replace the coupling-constant schematic combinations  $g_w g_s$  and  $g_w^2$  in these figures, respectively.

Since the momentum  $p_f \approx 420$  MeV/c of each of the final neutrons in Fig. 2(a) is much larger than the Fermi momentum of the initial neutron, the  $\Lambda$  hypernuclear decay rate induced by this diagram is well approximated by a quasi-free expression [30, 31]

$$\Gamma_n = v_{\Lambda n} \sigma_{\Lambda n \rightarrow nn} \rho_n, \quad (25)$$

where  $\rho_n$  is the neutron density in nuclear matter. To calculate the  $\Delta\mathcal{S} = 1$  two-body reaction cross section  $\sigma_{\Lambda n \rightarrow nn}$  at LO, we use a contact-term interaction  $\delta_\lambda(\mathbf{r})$  as in Eq. (14) with unknown LEC strength  $C_1^{(\lambda)}$ . This LEC is determined by fitting the r.h.s. of Eq. (25) to  $\Gamma_n \approx \frac{1}{2}\Gamma_{hyp}$ , where the total hypernuclear decay rate  $\Gamma_{hyp}$  which is dominated by non-mesonic hypernuclear decay [12] is the inverse of the hypernuclear lifetime determined experimentally in medium-heavy hypernuclei [32, 33],  $\tau_{hyp} \approx 210$  ps. Following this

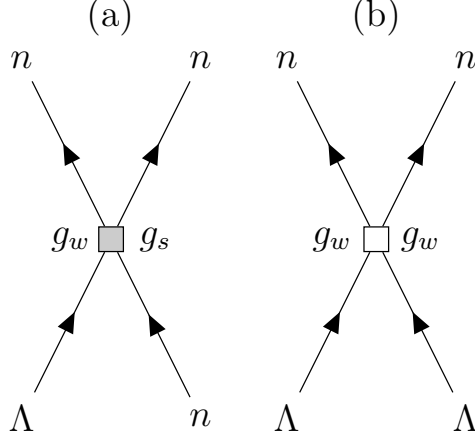


Figure 2:  ${}^1S_0 \rightarrow {}^1S_0$  LO EFT  $\Delta\mathcal{S} \neq 0$  weak-interaction diagrams: (a)  $\Delta\mathcal{S} = 1$   $\Lambda n \rightarrow nn$ , (b)  $\Delta\mathcal{S} = 2$   $\Lambda\Lambda \rightarrow nn$ .

approach for a representative value  $\lambda = 4 \text{ fm}^{-1}$ , and using a plane-wave (PW) approximation to evaluate  $\sigma_{\Lambda n \rightarrow nn}$  at rest, the value of the  $\Delta\mathcal{S} = 1$   ${}^1S_0 \rightarrow {}^1S_0$  LEC, up to a sign, is found to be

$$C_1^{(\lambda=4)} = -63.4 \text{ eV} \cdot \text{fm}^3, \quad (26)$$

with final-state interaction likely to increase it by up to a factor of two. Considering  $\Delta\mathcal{S} = 0$   ${}^1S_0$  LECs from Ref. [19]:  $C_0^{(\lambda=4)}(\Lambda N) = -239$  or  $C_0^{(\lambda=4)}(NN) = -301 \text{ MeV} \cdot \text{fm}^3$ , we note that the ratio  $C_1^{(\lambda=4)}/C_0^{(\lambda=4)}$  assumes values of  $2.65 \times 10^{-7}$  or  $2.11 \times 10^{-7}$ . These values are about the same ones obtained for  $g_w/g_s$  when (i)  $g_w$  is identified with the Fermi constant  $G_F m_\pi^2 = 2.21 \times 10^{-7}$  and (ii)  $g_s$  is of order one, well below the pion-exchange diagram value  $g_\pi \approx 13.6$ . In passing we note the weak dependence of  $C_1^{(\lambda)}$  on  $\lambda$ : choosing a shorter range parameter, say  $\lambda \sim 8 \text{ fm}^{-1}$  often practised in weak-interaction studies [29], results in  $C_1^{(\lambda=8)} = -51.5 \text{ eV} \cdot \text{fm}^3$ , a value smaller by 19% than in Eq. (26) for  $\lambda = 4 \text{ fm}^{-1}$ .

Once the  $\Delta\mathcal{S} = 1$  LEC  $C_1^{(\lambda)}$  has been determined, we multiply it by  $(g_w/g_s) \sim G_F m_\pi^2$  to estimate the required  $\Delta\mathcal{S} = 2$  LEC, yielding a value of  $C_2^{(\lambda)} = (2.21 \times 10^{-7})C_1^{(\lambda)}$ . Neglecting here too  $nn$  final-state interaction

(FSI), the  $H \rightarrow nn$  decay rate is given by

$$\Gamma(H \rightarrow nn) = \frac{\mu_{nn} k_n}{(2\pi\hbar c)^2} \int |\langle \exp(i\mathbf{k}_n \cdot \mathbf{r}) | C_2^{(\lambda)} \delta_\lambda(\mathbf{r}) | \tilde{\psi}_{\Lambda\Lambda}(r) \rangle|^2 d\hat{\mathbf{k}}_n. \quad (27)$$

Table 3:  $H \rightarrow nn$  decay rate  $\Gamma_H$ , Eq. (27), and  $H$  lifetime  $\tau_H = \hbar/\Gamma_H$  for several representative values of  $H$  binding energy  $B_{\Lambda\Lambda}$  and their associated neutron momentum release  $k_n$  values.

$B_{\Lambda\Lambda}$ (MeV)	$k_n$ (fm $^{-1}$ )	$\Gamma_H$ (eV)	$\tau_H$ (s)
176	2.109	$0.934 \cdot 10^{-19}$	$0.705 \cdot 10^4$
200	1.955	$0.873 \cdot 10^{-19}$	$0.754 \cdot 10^4$
300	1.130	$0.539 \cdot 10^{-19}$	$1.221 \cdot 10^4$

Calculated  $H \rightarrow nn$  decay rate values  $\Gamma_H$  and their associated lifetime values  $\tau_H$ , using a cutoff value  $\lambda = 4$  fm $^{-1}$  in Eq. (27), are listed in Table 3. A weak dependence of  $\tau_H$  on the  $H$  mass ( $m_H = 2m_\Lambda - B_{\Lambda\Lambda}$ ) is noted, in contrast with the strong dependence observed in Table 2 for the strong-interaction lifetime of  ${}_{\Lambda\Lambda}^6\text{He}$  caused by the rapid exponential decrease  $\exp(-a_\Phi^2 k_H^2)$  upon increasing  $k_H$  in Eq. (24). In the present case, the integral in Eq. (27) equals  $I(k_n; a_{\tilde{\psi},\lambda})$ , where the relatively large value  $a_\Phi \approx 1.5$  fm in Eq. (24) extracted from  ${}_{\Lambda\Lambda}^6\text{He}$  is replaced by a considerably smaller value  $a_{\tilde{\psi},\lambda} \lesssim 0.4$  fm owing to the considerably smaller size parameters of the deeply bound  $H$  wavefunction  $\tilde{\psi}$  and of the contact term  $\delta_\lambda(\mathbf{r})$ . The resulting integral  $I(k_n; a_{\tilde{\psi},\lambda})$  assumes then values about 10 fm $^3$  independently of  $k_n$ . Finally, the calculated  $H \rightarrow nn$  lifetimes are all of order  $10^4$  s, many orders of magnitude shorter than cosmological time scales commensurate with the age of the Universe. Regarding the model dependence of the above result,  $\tau_H \sim 10^4$  s, we note that introducing FSI in *both*  $\Gamma_n$  and  $\Gamma(H \rightarrow nn)$  calculations leads to almost the same decay rate  $\Gamma(H \rightarrow nn)$  as calculated using PW  $nn$  states, the reason being that the increased value of  $C_1^{(\lambda)}$  extracted then from  $\Gamma_n$  largely cancels the decrease of  $\Gamma(H \rightarrow nn)$  when FSI replaces PW. A further check is provided by the weak dependence on  $\lambda$ , the range parameter of  $C_1^{(\lambda)}$ , found in the final  $\Gamma(H \rightarrow nn)$  calculation.

## 6. Concluding remarks

In this work we considered hypernuclear constraints on the existence and lifetime of an hypothetical deeply-bound doubly-strange  $H$  dibaryon. Re-

garding the *existence* of  $H$ , it was found by considering the unambiguously identified  ${}_{\Lambda\Lambda}{}^6\text{He}$  double- $\Lambda$  hypernucleus that its strong-interaction lifetime for decay to  ${}^4\text{He} + H$  would increase substantially upon decreasing  $m_H$ , exceeding for  $m_H < m_\Lambda + m_n$  by far the  $10^{-10}$  s weak-interaction hypernuclear lifetime scale. Thus, the unique observation of double- $\Lambda$  hypernuclei through weak decay to single- $\Lambda$  hypernuclei does not rule out on its own the existence of a deeply-bound  $H$  dibaryon in the mass range  $2m_n$  to  $m_\Lambda + m_n$ , defying doubts raised by Dalitz et al. 35 years ago [11], but in agreement with the 20 years old claim by FZ [18]. Special attention was given in our evaluation to constrain hadronic cluster sizes by their binding energies and, indeed, our own conclusion follows from respecting the large difference between the r.m.s. radius of the loosely bound  $\Lambda\Lambda$  pair in  ${}_{\Lambda\Lambda}{}^6\text{He}$  and that of the compact  $\Lambda\Lambda$  pair within the  $H$  dibaryon. And furthermore, the anticipated  $\Lambda\Lambda$  short-range repulsion was fully considered by incorporating the SRC factor  $(1 - j_0(\kappa r))$ , Eq. (19), into the  $\Lambda\Lambda$  wavefunction.

If an  $H$ -like dibaryon existed in the mass range  $2m_n$  to  $m_\Lambda + m_n$ , its  $\Delta\mathcal{S} = 2$  decay lifetime  $\tau(H \rightarrow nn)$  would have been quite long, of the order of  $10^4$  s, but many orders of magnitude shorter than cosmological lifetimes comparable to the age of the Universe that  $H$  would need to qualify for a DM candidate. To reach this conclusion we used a weak-interaction EFT approach constrained by experimentally known, largely nonmesonic, hypernuclear lifetimes. Our conclusion is in stark disagreement with that reached by FZ [18] using somewhat outdated hard-core strong-interaction nuclear models and, furthermore, disregarding the constraint imposed on the  $H$  radius  $r_H$  by its binding energy.

We have not considered in the present work the case for an  $H$ -like dibaryon with mass below the  $nn$  threshold, a scenario likely to be ruled out by the established stability of several key nuclei, e.g.  ${}^{16}\text{O}$  [18]. A straightforward calculation of the hypothetical two-body decay rate  $\Gamma({}^{16}\text{O} \rightarrow H + {}^{14}\text{O})$  gives indeed a rate many orders of magnitude larger than established upper bounds for Oxygen. A report of this calculation is in preparation.

## Acknowledgements

Special thanks are due to Nir Barnea and Martin Schäfer for useful discussions during early stages of this work, and to Martin Schäfer for providing me with Table 1 based on our past joint hypernuclear studies. This work is

part of a project funded by the EU Horizon 2020 Research & Innovation Programme under grant agreement 824093.

## References

- [1] N. Aghanim, et al. (Planck Collab.), *Planck 2018 results*, Astronomy & Astrophysics 641 (2020) A6.
- [2] S. Gongyo, et al. (HAL QCD Collab.), *Most Strange Dibaryon from Lattice QCD*, Phys. Rev. Lett. 120 (2018) 212001.
- [3] J.R. Green, A.D. Hanlon, P.M. Junnarkar, H. Wittig, *Weakly Bound  $H$  Dibaryon from  $SU(3)$ -Flavor-Symmetric QCD*, Phys. Rev. Lett. 127 (2021) 242003, and references listed therein to earlier LQCD searches for a bound  $H$  dibaryon.
- [4] T. Inoue, et al. (HAL QCD Collab.), *Two-baryon potentials and  $H$ -dibaryon from 3-flavor lattice QCD simulations*, Nucl. Phys. A 881 (2012) 28.
- [5] J. Haidenbauer, U.-G. Meißner, *Exotic bound states of two baryons in light of chiral effective field theory*, Nucl. Phys. A 881 (2012) 44.
- [6] R.L. Jaffe, *Perhaps a stable Dihyperon*, Phys. Rev. Lett. 38 (1977) 195.
- [7] A.S. Carroll, et al., *Search for Six-Quark States*, Phys. Rev. Lett. 41 (1978) 777.
- [8] B.H. Kim, et al. (Belle Collaboration), *Search for an  $H$  Dibaryon with a Mass near  $2m_\Lambda$  in  $\Upsilon(1S)$  and  $\Upsilon(2S)$  Decays*, Phys. Rev. Lett. 110 (2013) 222002.
- [9] J. Adam, et al. (ALICE Collaboration), *Search for weakly decaying  $\bar{\Lambda}n$  and  $\Lambda\Lambda$  exotic bound states in central Pb-Pb collisions at  $\sqrt{s_{NN}}=2.76$  TeV*. Phys. Lett. B 752 (2016) 267.
- [10] J.P. Lees, et al. (BaBar Collaboration), *Search for a Stable Six-Quark State at BABAR*, Phys. Rev. Lett. 122 (2019) 072002.
- [11] R.H. Dalitz, D.H. Davis, P.H. Fowler, A. Montwill, J. Pniewski, J.A. Zakrzewski, *The identified  $\Lambda\Lambda$  hypernuclei and the predicted  $H$ -particle*, Proc. R. Soc. Lond. A 426 (1989) 1.

- [12] A. Gal, E.V. Hungerford, D.J. Millener, *Strangeness in nuclear physics*, Rev. Mod. Phys. 88 (2016) 035004.
- [13] E. Hiyama, K. Nakazawa, Annu. Rev. Nucl. Part. Sci. 68 (2018) 131.
- [14] J.K. Ahn, et al. (E373 KEK-PS Collaboration), *Double- $\Lambda$  hypernuclei observed in a hybrid emulsion experiment*, Phys. Rev. C 88 (2013) 014003.
- [15] A. Gal, *Comment on “Strangeness  $-2$  Hypertriton”*, Phys. Rev. Lett. 110 (2013) 179201.
- [16] G.R. Farrar, *A Stable  $H$ -Dibaryon: Dark Matter Candidate Within QCD?*, Int’l J. Theor. Phys. 42 (2003) 1211.
- [17] G.R. Farrar, Z. Wang, *Constraints on long-lived di-baryons and di-baryonic dark matter*, arXiv:2306.03123 [hep-ph] and references to earlier work cited therein.
- [18] G.R. Farrar, G. Zaharijas, *Nuclear and nucleon transitions of the  $H$  dibaryon*, Phys. Rev. D 70 (2004) 014008.
- [19] L. Contessi, M. Schäfer, N. Barnea, A. Gal, J. Mareš, *The onset of  $\Lambda\Lambda$  hypernuclear binding*, Phys. Lett. B 797 (2019) 134893.
- [20] L. Contessi, N. Barnea, A. Gal, *Resolving the  $\Lambda$  Hypernuclear Overbinding Problem in Pionless Effective Field Theory*, Phys. Rev. Lett. 121 (2018) 102502.
- [21] E. Hiyama, M. Kamimura, T. Motoba, T. Yamada, Y. Yamamoto, *Three-body model study of  $A = 6 - 7$  hypernuclei*, Phys. Rev. C 53 (1996) 2075.
- [22] T. Inoue (for the HAL QCD Collaboration), *Strange nuclear physics from QCD on lattice*, AIP Conf. Proc. 2130 (2019) 020002.
- [23] J. Maneu, A. Parreño, A. Ramos, *Effects of  $\Lambda\Lambda - \Xi N$  mixing in the decay of  $S = -2$  hypernuclei*, Phys. Rev. C 98 (2018) 025208.
- [24] N. Isgur, G. Karl, *Positive-parity excited baryons in a quark model with hyperfine interactions*, Phys. Rev. D 19 (1979) 2653,

- [25] G. Baym, *Lectures on Quantum Mechanics*, W.A. Benjamin 1969 (Library of Congress Catalog Card 68-5611), in particular Eq. (12-33) and related text.
- [26] K. Sasaki, et al. (HAL QCD Collab.),  *$\Lambda\Lambda$  and  $N\Xi$  interactions from lattice QCD near the physical point*, Nucl. Phys. A 998 (2020) 121737.
- [27] R.H. Dalitz, *50 years of hypernuclear physics*, Nucl. Phys. A 754 (2005) 14c.
- [28] A. Parreño, C. Bennhold, B.R. Holstein,  *$\Lambda N \rightarrow NN$  weak interaction in effective-field theory*, Phys. Rev. C 70 (2004) 051601(R); *An EFT for the weak  $\Lambda N$  interaction*, Nucl. Phys. A 754 (2005) 127c.
- [29] A. Pérez-Obiol, A. Parreño, B. Juliá-Díaz, *Constraints on effective field theory parameters for the  $\Lambda N \rightarrow NN$  transition*, Phys. Rev. C 84 (2011) 024606.
- [30] A. Gal, C.B. Dover, *Narrow  $\Sigma$ -Hypernuclear States*, Phys. Rev. Lett. 44 (1980) 379.
- [31] A. Gal, *Are  $\Sigma$  Nuclear States Really Narrow?*, Proc. Int'l. Conf. on Hypernuclear and Kaon Physics (Heidelberg, Germany, MPI H -1982 - V 20, edited by B. Povh) pp. 27-36.
- [32] Y. Sato, et al. (KEK-PS E307 Collaboration), *Mesonic and nonmesonic weak decay widths of medium-heavy  $\Lambda$  hypernuclei*, Phys. Rev. C 71 (2005) 025203.
- [33] X. Qiu, L. Tang, et al. (HKS JLab E02-017 Collaboration), *Lifetime of heavy hypernuclei*, Nucl. Phys. A 973 (2018) 116.